Linearly polarized second harmonic generation microscopy reveals chirality

V. K. Valev,[1]*, A. V. Silhanek[2], N. Smisdom[3], B. De Clercq[3], W. Gillijns[2], O. A. Aktsipetrov[4], M. Ameloot[3], V. V. Moshchalkov[2], and T. Verbiest[1]

[1] *Molecular Electronics and Photonics, INPAC, Katholieke Universiteit Leuven, Celestijnenlaan 200 D, B-3001 Leuven, Belgium.*

[2] *Nanoscale Superconductivity and Magnetism, Pulsed Fields Group, INPAC, Katholieke Universiteit Leuven, Celestijnenlaan 200 D, B-3001 Leuven, Belgium.*

[3] *University Hasselt and transnational University Limburg, BIOMED, Agoralaan building C, B-3590 Diepenbeek, Belgium.*

[4] *Department of Physics, Moscow State University, 11992 Moscow, Russia*

*v.k.valev@fys.kuleuven.be

http://www.valev.org

Abstract: In optics, chirality is typically associated with circularly polarized light. Here we present a novel way to detect the handedness of chiral materials with linearly polarized light. We performed Second Harmonic Generation (SHG) microscopy on G-shaped planar chiral nanostructures made of gold. The SHG response originates in distinctive hotspots, whose arrangement is dependent of the handedness. These results uncover new directions for studying chirality in artificial materials.

OCIS codes: (180.4315) Nonlinear Microscopy; (240.4350) Nonlinear optics at surfaces; (160.1585) Chiral media; (160.3918) Metamaterials

References and links

1. D. Schurig, J. J. Mock, B. J. Justice, S. A. Cummer, J. B. Pendry, A. F. Starr, and D. R. Smith, "Metamaterial electromagnetic cloak at microwave frequencies," Science **314**(5801), 977–980 (2006).
2. R. A. Shelby, D. R. Smith, and S. Schultz, "Experimental verification of a negative index of refraction," Science **292**(5514), 77–79 (2001).
3. J. B. Pendry, "Negative Refraction," Contemp. Phys. **45**(3), 191–202 (2004).
4. V. G. Veselago, "The Electrodynamics of substances with simultaneously negative values of ε and μ," Sov. Phys. Usp. **10**(4), 509–514 (1968).
5. A. Grbic, and G. V. Eleftheriades, "Overcoming the diffraction limit with a planar left-handed transmission-line lens," Phys. Rev. Lett. **92**(11), 117403 (2004).
6. N. Fang, H. Lee, C. Sun, and X. Zhang, "Sub–Diffraction-Limited Optical Imaging with a Silver Superlens," Science **308**, 534 (2005).
7. O. A. Aktsipetrov, I. M. Baranova, E. D. Mishina, and A. V. Petukhov, "Lightning rod effect in surface-enhanced second-harmonic generation," JETP Lett. **40**, 1012–1015 (1984).
8. H. Rigneault, J. M. Lourtioz, C. Delalande, and A. Levenson, eds., *Nanophotonics* (ISTE, 2006).
9. M. L. Brongersma, and P. G. Kirk, *Surface Plasmon Nanophotonics,* (Springer, Dordrecht, 2007).
10. J. B. Pendry, "A chiral route to negative refraction," Science **306**(5700), 1353–1355 (2004).
11. E. Plum, J. Zhou, J. Dong, V. A. Fedotov, T. Koschny, C. M. Soukoulis, and N. I. Zheludev, "Metamaterial with negative index due to chirality," Phys. Rev. B **79**(3), 035407 (2009).
12. S. Zhang, Y.-S. Park, J. Li, X. Lu, W. Zhang, and X. Zhang, "Negative refractive index in chiral metamaterials," Phys. Rev. Lett. **102**(2), 023901 (2009).
13. V. A. Fedotov, P. L. Mladyonov, S. L. Prosvirnin, A. V. Rogacheva, Y. Chen, and N. I. Zheludev, "Asymmetric propagation of electromagnetic waves through a planar chiral structure," Phys. Rev. Lett. **97**(16), 167401 (2006).
14. T. Petralli-Mallow, T. M. Wong, J. D. Byers, H. I. Yee, and J. M. Hicks, "Circular dichroism spectroscopy at interfaces: a surface second harmonic generation study," J. Phys. Chem. **97**(7), 1383–1388 (1993).
15. M. M.. Kauranen, T. Verbiest, A. Persoons, E. W. Meijer, M. N. Teerenstra, A. J. Schouten, R. J. M. Nolte, and E. E. Havinga, "Chiral effects in the second-order optical nonlinearity of a poly(isocyanide) monolayer," Adv. Mater. **7**(7), 641–644 (1995).
16. J. D. Byers, H. I. Yee, and J. M. Hicks, "A second harmonic generation analog of optical rotatory dispersion for the study of chiral monolayers," J. Chem. Phys. **101**(7), 6233 (1994).
17. A. Bouhelier, M. Beversluis, A. Hartschuh, and L. Novotny, "Near-field second-harmonic generation induced by local field enhancement," Phys. Rev. Lett. **90**(1), 013903 (2003).
18. M. W. Klein, C. Enkrich, M. Wegener, and S. Linden, "Second-harmonic generation from magnetic metamaterials," Science **313**(5786), 502–504 (2006).

#122754 - $15.00 USD Received 14 Jan 2010; revised 5 Feb 2010; accepted 13 Feb 2010; published 5 Apr 2010

19. W. Fan, S. Zhang, K. J. Malloy, S. R. J. Brueck, N.-C. Panoiu, and R. M. Osgood, "Second harmonic generation from patterned GaAs inside a subwavelength metallic hole array," Opt. Express **14**(21), 9570–9575 (2006).
20. J. A. H. van Nieuwstadt, M. Sandtke, R. H. Harmsen, F. B. Segerink, J. C. Prangsma, S. Enoch, and L. Kuipers, "Strong modification of the nonlinear optical response of metallic subwavelength hole arrays," Phys. Rev. Lett. **97**(14), 146102 (2006).
21. M. W. Klein, M. Wegener, N. Feth, and S. Linden, "Experiments on second- and third-harmonic generation from magnetic metamaterials," Opt. Express **15**(8), 5238–5247 (2007).
22. T. Xu, X. Jiao, G. P. Zhang, and S. Blair, "Second-harmonic emission from sub-wavelength apertures: Effects of aperture symmetry and lattice arrangement," Opt. Express **15**(21), 13894–13906 (2007).
23. B. K. Canfield, S. Kujala, K. Laiho, K. Jefimovs, J. Turunen, and M. Kauranen, "Chirality arising from small defects in gold nanoparticle arrays," Opt. Express **14**(2), 950–955 (2006).
24. S. Kujala, B. K. Canfield, M. Kauranen, Y. Svirko, and J. Turunen, "Multipolar analysis of second-harmonic radiation from gold nanoparticles," Opt. Express **16**(22), 17196–17208 (2008).
25. S. Kujala, B. K. Canfield, M. Kauranen, Y. Svirko, and J. Turunen, "Multipole interference in the second-harmonic optical radiation from gold nanoparticles," Phys. Rev. Lett. **98**(16), 167403 (2007).
26. H. Husu, B. K. Canfield, J. Laukkanen, B. Bai, M. Kuittinen, J. Turunen, and M. Kauranen, "Chiral coupling in gold nanodimers," Appl. Phys. Lett. **93**(18), 183115 (2008).
27. V. K. Valev, N. Smisdom, A. V. Silhanek, B. De Clercq, W. Gillijns, M. Ameloot, V. V. Moshchalkov, and T. Verbiest, "Plasmonic ratchet wheels: switching circular dichroism by arranging chiral nanostructures," Nano Lett. **9**(11), 3945–3948 (2009).
28. T. Verbiest, K. Clays, and V. Rodriguez, *Second-Order Nonlinear Optical Characterization Technique* (CRC Press, 2009).
29. E. Gielen, N. Smisdom, M. vandeVen, B. De Clercq, E. Gratton, M. Digman, J. M. Rigo, J. Hofkens, Y. Engelborghs, and M. Ameloot, "Measuring diffusion of lipid-like probes in artificial and natural membranes by raster image correlation spectroscopy (RICS): use of a commercial laser-scanning microscope with analog detection," Langmuir **25**(9), 5209–5218 (2009).
30. V. A. Fedotov, A. S. Schwanecke, N. I. Zheludev, V. V. Khardikov, and S. L. Prosvirnin, "Asymmetric Transmission of Light and Enantiomerically Sensitive Plasmon Resonance in Planar Chiral Nanostructures," Nano Lett. **7**(7), 1996–1999 (2007).
31. Y. Zeng, W. Hoyer, J. Liu, S. W. Koch, and J. V. Moloney, "Classical theory for second-harmonic generation from metallic nanoparticles," Phys. Rev. B **79**(23), 235109 (2009).
32. G. Bachelier, I. Russier-Antoine, E. Benichou, C. Jonin, and P.-F. Brevet, "Multipolar second-harmonic generation in noble metal nanoparticles," J. Opt. Soc. Am. B **25**(6), 955 (2008).
33. W. L. Schaich, "Second harmonic generation by periodically-structured metal surfaces," Phys. Rev. B **78**(19), 195416 (2008).
34. T. Verbiest, M. Kauranen, J. J. Maki, M. N. Teerenstra, A. J. Schouten, R. J. M. Nolte, and A. Persoons, "Linearly polarized probes of surface chirality," J. Chem. Phys. **103**(18), 8296–8298 (1995).
35. J. J. Maki, T. Verbiest, M. Kauranen, S. Van Elshocht, and A. Persoons, "Comparison of linearly and circularly polarized probes of second-order optical activity of chiral surfaces," J. Chem. Phys. **105**(2), 767–772 (1996).

Introduction

Artificial materials possess electromagnetic or optical properties that can be engineered to achieve unusual phenomena, such as cloaking [1], negative refraction [2,3] or super-lensing [5,6]. They are often referred to as "metamaterials", where the prefix *meta,* Greek for "beyond" or "after", suggests that the material exhibits characteristics surpassing those available in nature. This enhancement of physical properties frequently originates in an augmentation of the field intensity, occurring in a confined nanoscale region around the particles, which can reach several orders of magnitude. Two main phenomena are responsible for this localized field magnification. On the one hand, the electrostatic lightning-rod effect, which takes place at the geometric singularity of sharp curvatures where field lines become crowded [7], and, on the other hand, the surface plasmon resonances [8,9]. The latter constitute collective oscillations of the electrons that result in localized charge accumulation. This process is strongly affected by the nanostructures' geometry, by their dielectric properties and by the refractive index of the surroundings.

Chirality, the handedness of nature, is a key parameter for optical metamaterials and, as such, it has been the subject of intense research [10–13]. However, most studies so far have been made with linear optical techniques, while nonlinear probes are known to be typically much more sensitive to chirality, especially at the nanoscale [14–16].

Among the nonlinear optical phenomena, Second Harmonic Generation (SHG) holds a privileged position since it is the first and generally the largest contribution. It is well known for its surface and interface sensitivity down to the atomic submonolayer scale, which favors greatly the technique for probing nanostructures where the surface to volume ratio is among

#122754 - $15.00 USD Received 14 Jan 2010; revised 5 Feb 2010; accepted 13 Feb 2010; published 5 Apr 2010

the largest. Consequently, there is a growing interest in applying SHG to nanoparticles and nanopatterned materials [17–26].

Recently, it has been demonstrated with SHG microscopy that circularly polarized light can excite chiral plasmon modes, resulting in ratchet wheel-shaped SHG source patterns [27]. The direction of rotation in these ratchet wheels reveals the handedness of the material upon illumination with circularly polarized light. Indeed, in optics, chirality has generally been associated with *circularly* polarized light.

Here we show a novel way to observe chirality in optical materials, which involves *linearly* polarized light. We have applied SHG microscopy to an array of G-shaped planar nanostructures made of gold and found out that, surprisingly, linearly polarized fundamental radiation also can excite chiral and enantiomerically sensitive plasmon modes. SHG is emitted by clearly identifiable hotspots and the associated SHG source patterns are even more dramatically distinguishable, with respect to the handedness of the material, than upon using circularly polarized light.

Theory

For intense electromagnetic fields, in the electric dipole approximation, the induced polarization at the second harmonic frequency is given by $P_i^{NL}(2\omega) = \chi_{ijk}^{(2)} E_j(\omega) E_k(\omega)$, where ω is the frequency of the incident radiation, *i*, *j* and *k* are the Cartesian indices, $\chi_{ijk}^{(2)}$ is the second order susceptibility tensor and $E(\omega)$ the electric field component of the fundamental light. It can be seen that $\chi_{ijk}^{(2)}$ is responsible for the symmetry dependence of the SHG effect, since upon applying an inversion symmetry the vector quantities **P** and **E** change sign and as a consequence $\mathbf{P}^{NL} = \chi^{(2)}\mathbf{E}(\omega)\mathbf{E}(\omega)$ transforms into $-\mathbf{P}^{NL} = \chi^{(2)}[-\mathbf{E}(\omega)][-\mathbf{E}(\omega)]$. Therefore the nonlinear susceptibility has to be zero. Consequently, SHG is forbidden in centrosymmetric materials and can only appear in the regions of broken symmetry such as surfaces, interfaces, chiral ordering, etc [28]. In general, the number of independent components of the third rank tensor $\chi_{ijk}^{(2)}$ is completely determined by the symmetry. Thus, for a chiral 4-fold symmetric structure such as the one in Figs. 1a and 1b, the only non-vanishing components are $\chi_{xzz} = \chi_{yzz}$, $\chi_{xxz} = \chi_{yyz}$, χ_{zzz} and $\chi_{xyz} = -\chi_{yxz}$. This last component is often referred to as the "chiral" one, since it is characteristic of the absence of mirror symmetry that is associated with chiral systems. The other components are referred to as "achiral" because they occur in both chiral and achiral systems. It should be noted that for fundamental light incoming along the normal direction, all the susceptibility components containing at least one z index, should be zero. However, in the case of SHG microscopy, due to the strong focusing with the 100x objective, a large part of the incident electromagnetic radiation reaches the sample at a significant angle and henceforth all the tensor components contribute to the signal.

Experiments

The investigated samples consist of a periodic array of G-shape microstructures made of a Au(25 nm) layer thin-film evaporated by DC sputtering system on top of a Si/SiO_2 substrate. For the sample preparation we first cover the substrate with a double polymethyl metacrylate-methyl metacrylate resist layer in which the array of G-shaped and mirror-G-shaped structures are defined by electron-beam lithography. After the Au deposition, the resist is removed by a lift-off procedure involving sonication and/or boiling in acetone. The double resist layer has an overhanging profile which avoids any contact of the deposited material on top of the resist with the nanostructure themselves. Figures 1a and 1b shows a schematic diagram of the two chiral structures investigated. The lateral size of each individual motif is 1 μm wide, the line

#122754 - $15.00 USD Received 14 Jan 2010; revised 5 Feb 2010; accepted 13 Feb 2010; published 5 Apr 2010

width is 200 nm and the separation between neighboring structures is 200 nm. The whole array covers an area of 2.5×2.5 mm^2 and consists of $3,333 \times 3,333$ structures.

SHG microscopy images were collected with a confocal laser scanning microscope, Zeiss LSM 510 META (Jena, Germany). The sample was illuminated by a Tsunami femtosecond pulsed Ti:Sapphire laser, pumped by a 5 W Nd:YVO_4 laser, directed to the sample by a dichroic mirror (HFT KP650) and a Zeiss alpha PLAN-apochromat 100x/1.46 oil immersion objective. The fundamental excitation wavelength was 800 nm. The SHG-signal was collected by photomultiplier tubes via a NFT545 dichroic mirror and a KP685 short-pass filter that came with the confocal microscope. The scanning speed was set to a pixel dwell time of 102.4 µs with the image resolution set to 512-by-512 pixels. Each line was scanned twice and averaged. Total frame acquisition time was 63 s. The pinhole diameter was set to the maximum value, since optical sectioning was achieved through the multi-photon effect. The working distance of the 100x objective extended to 170 µm. Other details can be found in Ref. 29.

Results

Upon imaging the samples with SHG microscopy, for linearly polarized light, it can be observed that the nonlinear optical response originates in hotspots with different brightness, see Fig. 1c. The color coded intensities increase from purple, through green, then yellow to red. The direction of linear polarization is indicated by a white arrow. We can distinguish a planar chiral N-shaped pattern of hotspots. Noticing the scale in these figures, we observe that the dimensions of a single N pattern correspond to the size of a unit cell constituted of four G elements. The handedness of the material can therefore be directly deduced by looking at the SHG microscopy images. Furthermore, since different plasmon patterns are excited in the two types of structures, by comparing pixel brightness from the unit cells in Figs. 1c and 1d, one can also judge the handedness.

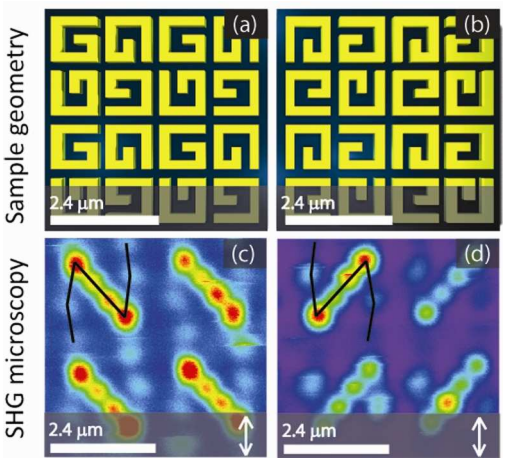

Fig. 1. Schematic diagram of the sample geometry of the G-shaped and of the mirror-G shaped sample structures, in a) and b) respectively. In c) and d), the SHG microscopy images of the G-shaped and of the mirror-G shaped sample structures respectively. The white arrows indicate the direction of the linear polarization. The color coded intensities increase from purple, through green, then yellow to red.

Interestingly, upon imaging the sample with opposite handedness, the N-shaped SHG pattern reverses to a mirror-N shaped one, see Fig. 1d. Especially, the bright “hot spots” are aligned along different directions depending on the handedness of the material.

#122754 - $15.00 USD Received 14 Jan 2010; revised 5 Feb 2010; accepted 13 Feb 2010; published 5 Apr 2010

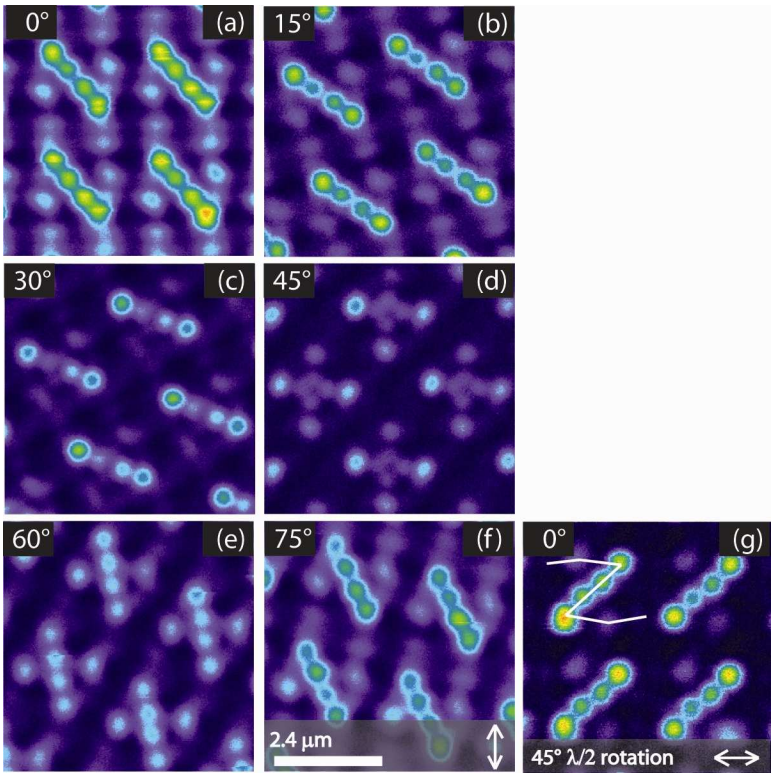

Fig. 2. In a), b), c), d), e) and f), the SHG microscopy images of the G-shaped sample structures (Fig. 1a) as a function of the sample position angle, in degrees, on the microscope stage. Orientation a) corresponds to that in Fig. 1a. In g), a SHG microscopy image of the same structures positioned at 0°, with the incoming polarization rotated 90° by means of a half wave plate. The white arrows indicate the direction of the linear polarization. Images a) – f) have the same polarization of the incoming beam. The color coded intensities increase from purple, through green, then yellow to red.

In order to verify that the handedness of the N-shaped SHG patterns is indeed related to the chirality of the Gs and is not solely due to anisotropy, the SHG microscopy response was followed as function of sample rotation angle on the microscope stage. As it is well known, chirality is unaffected by rotation while anisotropy is not. Therefore, should anisotropy be the only reason for the difference in patterns observed in Figs. 1c and 1d then, upon rotating the samples, at some orientation, the patterns should have become superimposable one upon the other. Figures 2a to 2f show that the SHG hotspots revolve in a manner that conserves the handedness of the N-shaped patterns. Consequently, its reversal in Figs. 1d can only be attributed to the handedness of the Gs. Please note that the 90° image is not shown in Fig. 2 in order to avoid redundancy, since it is essentially the same as that at 0°. It should also be noted that the bright spots do rotate 90° upon rotating the incoming polarization at 90° while the sample remains at 0° orientation, see Fig. 2g. This is due to the excitation of enhanced surface plasmon resonances in different points of the nanostructures. However, while the overall pattern rotates 90° its chirality remains unaffected as can be established by observing the handedness of the N-shaped patterns between Figs. 1d and 2g.

#122754 - $15.00 USD Received 14 Jan 2010; revised 5 Feb 2010; accepted 13 Feb 2010; published 5 Apr 2010

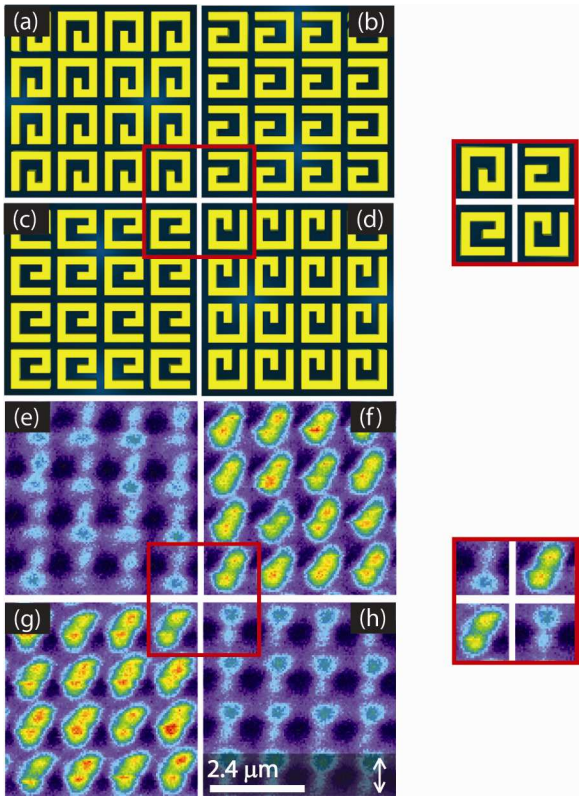

Fig. 3. In a), b), c) and d), schematic diagram of the sample geometry of the mirror-G shaped sample structures rotated in steps of 90°. In e), f), g) and h), the corresponding SHG microscopy images. The color coded intensities increase from purple, through green, then yellow to red. The red squares emphasize the pattern reproducing the mirror-G unit cell in Fig. 1. The white arrows indicate the direction of the linear polarization, which is identical for all images shown.

The origin of the N-shaped pattern in the SHG micrographs can be understood upon imaging a sample, where the individual spiral elements are arranged in identical rows and columns, as shown in Fig. 3. Rotating such a sample in steps of 90° as it is shown in Figs. 3a to 3d reproduces the unit cell in Fig. 1b. In Fig. 3 this unit cell is emphasized with a red square. The SHG microscopy pictures corresponding to the above sample positions respectively are displayed in Figs. 3e to 3h. The scale of the pictures being the same as in Fig. 1, we notice that with each individual G structure are associated two SHG hotspots. While these are dark in the case of Figs. 3e and 3h, they become much brighter in Figs. 3f and 3g. Furthermore, within the darker hotspots, the lower one is larger than in Fig. 3e while in Fig. 3h it is the higher one that is larger. All of these individual features can be seen in the red square that connects the SHG micrographs and they are identical to the ones composing the pattern in Fig. 1d. Therefore, it can be assumed that the SHG response in the case of Fig. 1 is the result of juxtaposing the SHG responses from each individual component. This leads us to the conclusion that in the case of linearly polarized light, the SHG microscopy is capable of distinguishing the handedness at the level of each individual G.

Recently, the G-structures discussed here where also investigated by circularly polarized SHG microscopy. We would like to point out that the experiments discussed here are fundamentally different from the results obtained in Ref. 27. The reason is that, for individual structures, there is no visible distinction in the SHG hotspot pattern, which is observed for left- and right-hand circularly polarized light (see Figs. 3c and 3d in Ref. 27). Consequently, there seems to be an essential difference in the plasmon modes excited by circularly or

#122754 - $15.00 USD Received 14 Jan 2010; revised 5 Feb 2010; accepted 13 Feb 2010; published 5 Apr 2010

linearly polarized light, since in the former case plasmon modes appear to propagate between structures and exhibit sensitivity to the chirality of the four Gs unit cell while in the latter case the plasmon modes are confined to the individual Gs and chirality is detected at the level of single structures. However, further work is needed to clarify this difference. Furthermore, while discrimination between different enantiomers by means of circularly polarized light is well-known, we here show that this is also possible by means of linearly polarized light, independently of the polarization direction.

The SHG hotspots originate, most likely, in the surface plasmon resonance field enhancement of the nanostructures. The presence of such a resonance near 800 nm was experimentally verified. In Fig. 4 the SHG microscopy images as function of the excitation wavelength and power are displayed for a sample having a structure and an orientation identical to that in Fig. 3b. Note that the laser power was measured before the beam entered the microscope. Furthermore, since we are only interested in the intensity of the signal, the scale in these micrographs is larger than in the previous ones. The maximum of SH generation is found to be between 790 and 800 nm (Figs. 4c and 4d respectively), while for 780 and 810 nm the signal drops dramatically (see Figs. 4b and 4e) and, finally, at 770 and 820 it almost completely disappears (see Figs. 4a and 4f) even though the excitation power for these last two micrographs was more than doubled.

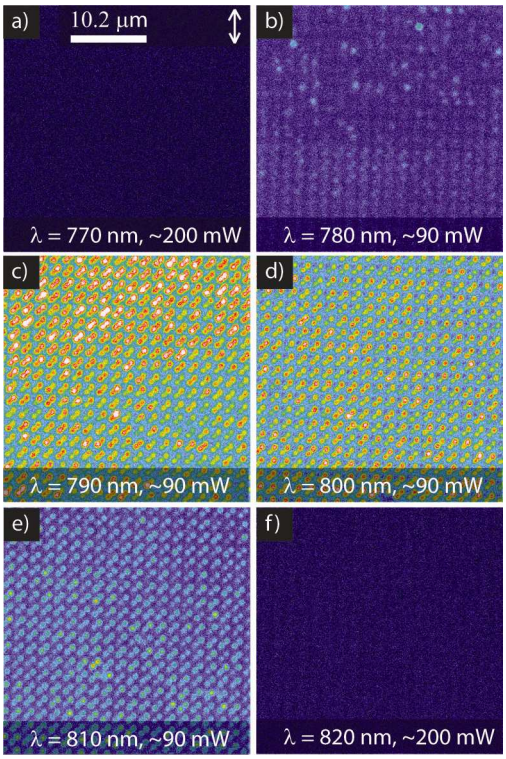

Fig. 4. In a) to f) SHG microscopy images of the G-shaped sample structures as function of increasing fundamental wavelength from 770 nm to 820 nm in steps of 10 nm. The color coded intensities increase from purple, through green, then yellow to red. The white arrows indicate the direction of the linear polarization.

The presence of this very sharp resonance near 800 nm suggests that the second harmonic light is most likely generated from the regions of high charge accumulation or in the places of strong field-enhancement due to the lightning-rod effect. Its sensitivity to chirality can then be attributed to enantiomerically sensitive plasmon modes, which were already observed in linear optics [30], and which could be related to the SHG response through recent theoretical studies [31–33].

#122754 - $15.00 USD Received 14 Jan 2010; revised 5 Feb 2010; accepted 13 Feb 2010; published 5 Apr 2010

We wish to emphasize that the effect which we present here is fundamentally different from SHG – Optical Rotation or SHG – Linear Dichroism. In the latter the SHG response has a different intensity for positive (45° or −135°) and negative (135° or −45°) polarization state of the pump beam [34,35]. Both these phenomena depend on well defined incoming and outgoing polarization states. In our experiment, we demonstrate that we can distinguish chirality with linearly polarized light, independently of the polarization direction and the polarization state of the SH-light.

Conclusions

In summary, we presented a novel way of observing chirality in optical metamaterials using linear polarized light in SHG microscopy. The latter was shown to constitute a valuable tool for mapping the electromagnetic fields in chiral optical metamaterials. We believe that our work will stimulate further investigations of chiral optical metamaterials with nonlinear optics. Variations in size, shape and materials of our structures will likely exhibit a multitude of interesting patterns and properties.

Acknowledgments

We acknowledge financial support from the fund for scientific research Flanders (FWO-V), the University of Leuven (GOA), Methusalem Funding of the Flemish Government and the Belgian Inter-University Attraction Poles IAP Programs. V. K. V., A. V. S. and W. G. are grateful for the support from the FWO-Vlaanderen. N. S. and B. D. C. acknowledge the Instituut voor de Aanmoediging van Innovatie door Wetenschap en Technologie in Vlaanderen. O.A.A. acknowledges the financial support from the Russian Foundation for Basic Research.

#122754 - $15.00 USD Received 14 Jan 2010; revised 5 Feb 2010; accepted 13 Feb 2010; published 5 Apr 2010